SCIENCE CHINA
Information Sciences

• **RESEARCH PAPER** •

November 2014, Vol. 57 112202:1–112202:13
doi: 10.1007/s11432-014-5135-3

Biologically adaptive robust mean shift algorithm with Cauchy predator-prey BBO and space variant resolution for unmanned helicopter formation

WANG XiaoHua & DUAN HaiBin*

State Key Laboratory of Virtual Reality Technology and Systems, Beihang University, Beijing 100191*, China*

Received December 27, 2013; accepted April 2, 2014; published online June 16, 2014

Abstract Visual tracking technology can provide measurement information for unmanned helicopter formation and thus, more attention is being paid to this research area. We propose a novel mean shift (MS) algorithm that is both adaptive and robust for unmanned helicopter formation and apply it to the leading unmanned helicopter tracking. The movement of an unmanned helicopter is very flexible and changeable, which makes the tracking there of more difficulty than for common targets. In creating an algorithm that can adapt to the acceleration of the unmanned helicopter and estimates both the scale and orientation of the movement changes, we combine the traditional MS with the bio-inspired Cauchy predator-prey biogeography-based optimization (CPPBBO) evolutionary algorithm, and also the space variant resolution (SVR) mechanism of the human visual system (MS-CPPBBO-SVR). To demonstrate the effectiveness and robustness of the proposed method and justify the importance of the CPPBBO algorithm and SVR mechanism at the same time, a series of comparative experiments were carried out. The experimental results of the proposed MS-CPPBBO-SVR method are compared with other competitive tracking methods, such as MS, MS with SVR (MS-SVR), MS-SVR with several other optimization algorithms, and the robust particle filter algorithm. The experimental results demonstrate that our proposed tracking approach, MS-CPPBBO-SVR, is more adaptive, robust and efficient in target tracking than the other methods.

Keywords unmanned helicopter, formation, tracking, mean shift, biogeography-based optimization (BBO), predator-prey, space variant resolution (SVR)

Citation Wang X H, Duan H B. Biologically adaptive robust mean shift algorithm with Cauchy predator-prey BBO and space variant resolution for unmanned helicopter formation. Sci China Inf Sci, 2014, 57: 112202(13), doi: 10.1007/s11432-014-5135-3

1 Introduction

The use of unmanned aerial vehicles (UAVs) has recently aroused much interest in civil and industrial markets [1] because of the advantages of zero casualties, high-speed overload, good stealth performance, short operational preparation time, and relatively low life-cycle cost [2]. Multiple-UAVs moving in formation have attracted even more attention [3–8]. As visual tracking technology can obtain the state parameters of the target, it can be applied to UAV formation. With the information extracted by the

*Corresponding author (email: hbduan@buaa.edu.cn)

visual system, the following unmanned helicopters can ascertain the direction and distance of the leader, thereby providing measurement information for the control and management of UAV formation. Of the various types of UAVs, small-scale unmanned helicopter can serve as an excellent platform for studying vehicles with maneuverability and versatility as these can be seamlessly manipulated in manual mode and easily operated in automatic mode [9–12]. The aim of this study is to design an adaptive, robust and efficient method that can be applied to UAV formation. Unmanned helicopters are used to verify the superiority of the proposed method. In a leader-wingman formation pattern the visual tracking system is embedded in the wingman, while the leader is the target for tracking. In this case, the helicopters fly in the expected formation pattern. However, tracking an unmanned helicopter is more difficult than other common targets as it can move quickly and can suddenly change its speed, in addition to the rotation and scaling there. In addition, the working environment of an unmanned helicopter can be very complex, which undoubtedly increases the difficulty of tracking. Hence, tracking results can be used to demonstrate convincingly the effectiveness of the tracking methods.

Numerous efficient tracking algorithms have been proposed. Mean shift (MS) [13], which is a simple iterative procedure for estimating the gradient of a density function, is one of the most popular owing to its simplicity and effectiveness. However, the premise for using the classic MS tracker is that the movement of the target between frames is relatively small and smooth. Thus, the basic MS tracker is easily prone to local minima if the target (the leading unmanned helicopter in this paper) moves rapidly or the background changes noticeably. Moreover, scale and orientation changes in the target can also lead to poor tracking performance of the MS. Hence, many improved versions of MS tracker [14–18] have been proposed to enhance the robustness there.

The advantages of bio-inspired intelligence are high robustness, good distributed computing mechanisms, and the ease with which it can be combined with other methods [19]. In this paper, we include such intelligence in the classic MS tracker, thereby making the tracker robust and adaptive. A hybrid mean shift method based on the Cauchy predator-prey [20] biogeography-based optimization (CPPBBO) and space variant resolution (SVR) [21] (MS-CPPBBO-SVR) is presented to overcome the disadvantages of the basic MS tracker especially when used for tracking the leading unmanned helicopter in formation.

The proposed CPPBBO algorithm is an improved version of biogeography-based optimization (BBO), which is a new optimization algorithm proposed by Simon [22]. CPPBBO incorporates the concept of predator-prey in basic BBO and uses a new mutation operator based on the Cauchy operator to improve its capability of searching for optimal solutions. SVR is a mechanism that describes the mapping from the human retina to the striate cortex.

There are two advantages of the proposed biologically MS-CPPBBO-SVR tracking method. One is that the CPPBBO algorithm is applied to search for a better starting position in a larger range to obtain a better target candidate for the MS tracker. The other is that the SVR mechanism is introduced to help the tracker ascertain the scale and rotation information of the target and at the same time reduce the computational cost. Experimental results show that the proposed novel tracking method MS-CPPBBO-SVR is adaptive, more robust and efficient in tracking the leading unmanned helicopter in an unmanned helicopter formation.

2 Classic mean shift for visual tracking

The MS tracking method uses kernel color histograms as the tracking feature and the Bhattacharyya coefficient to measure the similarity between the target model and candidate regions.

Let $\{x_i^s\}_{i=1,2,\dots,n}$ denote the pixel locations of a given target centered at x_0 in the initial frame of the sequence. The kernel function $k(x)$ with the object bandwidth h is used in the kernel color histogram [23] of the target model, which is given by

$$\hat{q}_u = C\sum_{i=1}^{n} k\left(\left\|\frac{x_0 - x_i^s}{h}\right\|^2\right)\delta\left[b\left(x_i^s\right) - u\right] \quad (u = 1,\dots,m), \tag{1}$$

where h is the object bandwidth. If the size of the target is $a\times b$, $h=\sqrt{a^2+b^2}$. $C=[\sum_{i=1}^{n}k(\|\frac{x_0-x_i^s}{h}]\|^2)]^{-1}$ is the normalization constant obtained by imposing the condition $\sum_{u=1}^{m}\hat{q}_u=1$. Furthermore $\delta(x)$ is Kronecker's delta function with the index of the histogram bin u, while $b(x)$ is the kernel color histogram bin index function. Let $g(x)=-k'(x)$; then, the corresponding kernel is defined as $G(x)=g\left(\|x\|^2\right)$.

Similarly, the pixel locations of the target candidate centered at y are denoted by $\{y_i\}_{i=1,2,\ldots,n}$. The color histogram of the target candidate can be obtained by

$$\hat{p}_u(y)=C_h\sum_{i=1}^{n_h}k\left(\left\|\frac{y-x_i}{h}\right\|^2\right)\delta\left[b\left(x_i\right)-u\right]\quad(u=1,\ldots,m), \tag{2}$$

where the normalization constant

$$C_h=\frac{1}{\sum_{i=1}^{n_h}k(\left\|\frac{y-x_i}{h}\right\|^2)} \tag{3}$$

is derived by imposing the condition

$$\sum_{u=1}^{m}\hat{p}_u(y)=1. \tag{4}$$

The Bhattacharyya coefficient, which is taken as a measurement of the similarity between the tracking target (the leading unmanned helicopter) model and the candidate, is defined as

$$\hat{\eta}(y)\equiv\eta\left[\hat{p}(y),\hat{q}\right]=\sum_{u=1}^{m}\sqrt{\hat{p}_u(y)\hat{q}_u}. \tag{5}$$

The distance between the model and the candidate can be obtained by

$$d(y)=\sqrt{1-\eta\left[\hat{p}(y),\hat{q}\right]}=\sqrt{1-\sum_{u=1}^{m}\sqrt{\hat{p}_u(y)\hat{q}_u}}. \tag{6}$$

The degree of similarity is the highest when $d(y)$ is at its minimum and at the same time η is at its maximum.

With a Taylor expansion around the values $\hat{p}_u(y_0)$, where y_0 is the estimated location of the leading unmanned helicopter in the previous frame, the Bhattacharyya coefficient can be approximated as

$$\eta[\hat{p}(y),\hat{q}]\approx\frac{1}{2}\sum_{u=1}^{m}\sqrt{\hat{p}(y),\hat{q}_u}+\frac{C_h}{2}\sum_{i=1}^{n}w_ik\left(\left\|\frac{y-x_i}{h}\right\|^2\right), \tag{7}$$

where

$$w_i=\sum_{u=1}^{m}\delta[b(x_i)-u]\sqrt{\frac{\hat{q}_u}{\hat{p}_u(y_0)}}. \tag{8}$$

The maximum of the second part of (7) can be calculated by iterative mean shift with kernel $G\left(x\right)$ along the gradient direction.

The current location y_1 is computed by the following iteration

$$y_1=\frac{\sum_{i=1}^{m}x_iw_ig(\left\|\frac{y_0-x_i}{h}\right\|^2)}{\sum_{i=1}^{m}w_ig(\left\|\frac{y_0-x_i}{h}\right\|^2)}, \tag{9}$$

where

$$w_i=\sum_{u=1}^{m}\delta[b(x_i)-u]\sqrt{\frac{\hat{q}_u}{\hat{p}_u(y_0)}}. \tag{10}$$

In the iteration of the MS procedure, w_i and y_1 are computed. Then, y_1 replaces y_0 to obtain the new location y_2. The above two steps are repeated until $\|y_k-y_{k-1}\|$ is smaller than the pre-set positive value or the number of iteration k is greater than a predetermined maximum. The output y_k is the location of the leading unmanned helicopter in the current frame.

3 Principles of the CPPBBO algorithm

3.1 The basic BBO algorithm

BBO, which is based on mathematic models of biogeography, is a stochastic optimization technique inspired by the geographical distribution and migration of species in an ecosystem. In the BBO algorithm, a set of habitats is used to represent the possible solutions, with a suitability index variable (SIV) describing the feature of each habitat, and a habitat suitability index (HSI) is the evaluation criteria to measure the quality of a solution. BBO works mainly based on two mechanisms, migration and mutation. Suppose that there is a habitat H with a vector of SIVs; by following the migration and mutation steps, new candidate habitats are generated and the BBO algorithm can reach an optimal solution.

If there are$s$species in the habitat, immigration rate$\lambda$and emigration rateμcan be calculated by

$$\lambda_s = I\left(1 - \frac{s}{n}\right); \quad \mu_s = \frac{Es}{n}, \tag{11}$$

where I is the maximum immigration rate, E is the maximum emigration rate, and n is the greatest possible number of species that the habitat can support.

P_s is the probability that the habitat contains exactly s species, which changes from time t to time $t + \Delta t$ as follows:

$$P_s(t+\Delta t) = P_s(t)(1 - \lambda_s \Delta t - \mu_s \Delta t) + P_{s-1}\lambda_{s-1}\Delta t + P_{s+1}\mu_{s+1}\Delta t. \tag{12}$$

In classic BBO, the mutation rate $m(s)$ is simply given proportional to P_s as

$$m(s) = m_{\max}\left(1 - \frac{P_s}{P_{\max}}\right) \tag{13}$$

where $m_{\max}$ is a user-defined parameter, and $P_{\max}$ is the maximum species count probability.

3.2 Proposed CPPBBO algorithm

The proposed CPPBBO is an optimization algorithm that uses a new mutation operator based on the Cauchy operator and incorporates the concept of predator-prey in classic BBO to increase the diversity of the population and overcome the problem of local optimum traps.

The probability density function of a Cauchy distribution with location parameter 0 and scale parameter 1 is given as

$$f(x; 0, 1) = \frac{1}{\pi(1 + x^2)}. \tag{14}$$

Then, Cauchy mutation at $t = 1$ can be expressed as

$$H_i'(j) = \min(H_i) + (\max(H_i) - \min(H_i)) \times \pi \times f(H_i(j); 0, 1), \tag{15}$$

where $H_i(j)$ is the jth dimension variable of individual H_i and $f(H_i(j); 0, 1)$ indicates that a new Cauchy distributed number is generated for each individual of j.

In nature, predatory behavior is one of the most common phenomena. In the algorithm, the predator is modeled as

$$S_{\text{predator}} = S_{\text{worst}} + \zeta(1 - \text{Nc}/\text{Nc}_{\max}) \tag{16}$$

where S_{predator} is the solution chosen as the predator, and S_{worst} is the worst solution in the population. Nc is the current iteration, $\text{Nc}_{\max}$ is the total number of iterations, and ζ is the hunting rate, which is a particular given number.

Eq. (17) describes a model of prey fleeing and provides solutions for maintaining a safe distance from the predator.

$$\begin{cases} S_{\text{Nc}+1} = S_{\text{Nc}} + \zeta \mathrm{e}^{-|D|}, & D \geqslant 0, \\ S_{\text{Nc}+1} = S_{\text{Nc}} - \zeta \mathrm{e}^{-|D|}, & D < 0, \end{cases} \tag{17}$$

where D is the distance between the solution and the predator, and Nc is the current iteration.

In the CPPBBO algorithm a set of habitats is initialized according to the problem. The migration rates are iteratively used to modify each habitat, while Cauchy mutation is used to update the individuals. Thereafter, the habitat with the lowest HSI is chosen as the predator. Eqs. (16) and (17) are used to find the solutions. When an iteration terminates, the HSI of each habitat is updated and the habitat with the highest HSI is the solution.

3.3 Theoretical analysis of CPPBBO

A Markov chain model of basic BBO with selection, migration, and mutation operators was developed in [24]. The distribution of a BBO population can be represented by a Markov state. Suppose that the population size is N and the possible solutions are represented by x_i comprising q dimensions. If the range of the solutions is r, the cardinality of the search space is $S = r^q$. Here v denotes the population vector, and v_i is the number of x_i individuals in the population. $x_i(s)$ is the sth dimension of x_i, and $J_i(s) = \{j : x_j(s) = x_i(s)\}$.

A Markov model of the migration can be given as

$$\Pr(y_k(s)_{t+1} = x_i(s)) = (1 - \lambda_{m(k)})1_0(x_{m(k)}(s) - x_i(s)) \ + \lambda_{m(k)} \frac{\sum_{j\in J_i(s)} v_j u_j}{\sum_{j=1}^{n} v_j u_j}, \tag{18}$$

where $\lambda_{m(k)}$ is the probability of immigration to $y_k(s)$, and 1_0 is the indicator function of the set $\{0\}$.

$$P_{ki}(v) = \Pr(y_{k.t+1} = x_i) = \prod_{s=1}^{q} \Pr(y_k(s)_{t+1} = x_i(s)), \tag{19}$$

where $P_{ki}(v)$ denotes the probability that immigration results in $y_k = x_i$, and q is the dimension of the solution.

Let $\Pr(u|v)$ represent the probability that population vector u is obtained from v after a generation. Then,

$$\Pr(u|v) = \sum_{J\in Y} \prod_{k=1}^{N} \prod_{i=1}^{n} [P_{ki}(v)]^{J_{ki}}, \tag{20}$$

$$Y = \left\{ J \in \mathbb{R}^{N\times n} : J_{ki} \in \{0,1\}, \quad \sum_{i=1}^{n} J_{ki} = 1 \text{ for all } k, \quad \sum_{k=1}^{N} J_{ki} = u_i \text{ for all } i \right\}. \tag{21}$$

As the Cauchy operator does not affect the property of the Markov model for the mutation, it is the same as that of basic BBO and can be defined as

$$P_{ki}^{(2)}(v) = \sum_{j=1}^{n} U_{ij} P_{ki}(v), \quad P^{(2)}(v) = P(v)U^{\mathrm{T}}, \tag{22}$$

where U_{ij} denotes the probability that x_j mutates to x_i, and $P_{ki}^{(2)}(v)$ denotes the probability that the mutation following the kth immigration results in x_i. Then we have

$$\Pr^{(2)}(u|v) = \sum_{J\in Y} \prod_{k=1}^{N} \prod_{i=1}^{n} [P_{ki}^{(2)}(v)]^{J_{ki}}. \tag{23}$$

For the predator-prey mechanism in CPPBBO, V_{ij} is used to denote the probability that x_j flees to x_i.

$$P_{ki}^{(3)}(v) = \sum_{j=1}^{n} V_{ij} P_{ki}^{(2)}(v), \quad P^{(3)}(v) = P^{(2)}(v)V^{\mathrm{T}}, \tag{24}$$

where $P_{ki}^{(3)}(v)$ is the probability that the predator-prey following the kth immigration and mutation results in x_i.

From the above analysis, it is obvious that the new population is dependent only on the current population, which means that $\{x(n),\ n \in N\}$ is a discrete time Markov chain.

The global optimal solution set can be expressed as $M = \max(f(x_k),\ k = 1, 2, \ldots, S)$, where S is the cardinality of the search space.

Lemma 1. The evolution direction of the habitat of CPPBBO is unchangeable, i.e., $f(x_{i+1}) \geqslant f(x_i)$.

Proof. In each generation, a greedy selection operator is used to select a better solution and save the vector of the relevant habitat. At the same time, the elitism approach can save the features of the habitat with the best solution in the CPPBBO process, and the best solution can be reverted even if migration or mutation ruins the HSI.

Theorem 1. The CPPBBO algorithm converges to the global optimal solution set, $M \neq \emptyset$, with probability 1, i.e., $\lim_{n\to\infty} P(x(n) \in M) = 1$, which is independent of the initial distribution.

Proof. From Lemma 1, it is obvious that

$$P(x(n+1) \in M | x(n) \in M) = 1. \tag{25}$$

Suppose that $P(x(n+1) \in M | x(n) \notin M) = p(n) > 0$, which is feasible for most actual situations. The probability that no population enters the global optimal solution set after n iterations, $P_{\text{not}}(n)$ [25] can be calculated as follows:

$$P_{\text{not}}(n) = \prod_{t=1}^{n} (1 - p(t)). \tag{26}$$

Then

$$P(x(n) \in M) = 1 - P_{\text{not}}(n). \tag{27}$$

Suppose $n \to \infty$, then $\lim_{n\to\infty} P(x(n) \in M) = 1 - \prod_{t=1}^{\infty} (1 - p(t))$. As $0 < p(t) \leqslant 1$, $0 < 1 - p(t) \leqslant 1$. Thus

$$\prod_{t=1}^{\infty} (1 - p(t)) = 0, \tag{28}$$

$$\lim_{n\to\infty} P(x(n) \in M) = 1 - \prod_{t=1}^{\infty} (1 - p(t)) = 1. \tag{29}$$

The process used in the proof shows that the conclusion reached is independent of the initial population. Therefore, the CPPBBO algorithm can converge to the global optimal solution set, $M \neq \emptyset$.

4 Space variant resolution

The mapping from the human retina to the striate cortex is a space variant one that can be approximated by a complex log transformation with a high resolution in the foveal region and a decreasing one (low resolution) moving towards the periphery.

According to [26], any pixel point (x_i, y_i) in the image plane can be expressed in terms of (ρ, θ) in the retinal plane and (ξ_i, ψ_i) in the cortical plane. The log-polar transform is

$$\rho = \sqrt{(x_i - x_0)^2 + (y_i - y_0^2)}, \tag{30}$$

$$\theta = \arctan\left(\frac{y_i - y_0}{x_i - x_0}\right), \tag{31}$$

$$\xi_i = M \ln(\rho), \tag{32}$$

$$\psi_i = \theta, \tag{33}$$

where (x_0, y_0) is the origin of coordinates in the image plane, and M is a positive real number representing an adjustable parameter based on the dimensions of the receptive field and the desired mapping. θ is constrained to the range $[0, 2\pi)$. In particular, when $x_i = x_0,\ y_i = y_0,\ \psi_i$ and ξ_i are equal to zero.

While tracking the leading unmanned helicopter, it is necessary to focus on the target area. Hence, the space of the object variant resolution model can be defined as the target area transformed by the log-polar transform. In the log-polar plane, the shift values of the scale and rotation between the target area of the kth frame and that of the $(k-1)$th frame are denoted by $\Delta\xi^k,\ \Delta\psi^k$. The scale and rotation changes of the target in the retinal plane are, respectively, given as

$$S_k = \frac{\rho_k}{\rho_{k-1}} = \frac{\mathrm{e}^{\xi_k/M}}{\mathrm{e}^{\xi_{k-1}/M}} = \mathrm{e}^{\Delta\xi_k/M}, \tag{34}$$

$$r_k = (\theta_k - \theta_{k-1}) = (\psi_k - \psi_{k-1}) = \Delta\psi_k. \tag{35}$$

Here $(\rho_{k-1},\ \theta_{k-1})$ and (ρ_k, θ_k) are the coordinates of the target areas of the $(k-1)$th and kth frames in the retinal plane, respectively, and (ξ_{k-1}, ψ_{k-1}) and (ξ_k, ψ_k) are the transformed coordinates of the target areas in the log-polar plane, respectively.

5 The proposed biologically hybrid method

In the adaptive robust MS-CPPBBO-SVR algorithm, the proposed biologically CPPBBO algorithm is applied to conduct a global robust search in a larger neighborhood of the target position in the previous frame. Then, a local search can be conducted by the MS vector to obtain the best matching of the leading unmanned helicopter in the current frame. Furthermore, SVR is introduced to extract the scale and rotation information of the tracking window. Therefore, the tracking window is adaptive to changes in the target and the amount of computation is reduced. The implementation procedure is described below.

a) Manually define the leading unmanned helicopter for tracking in the first frame. Calculate the distribution of the leading unmanned helicopter model by (1). Compute the log-polar transform of the leading unmanned helicopter using (30)–(33).

b) For the next frame, use the CPPBBO algorithm to search for a better location y_m than $\hat{y}_0$ of the leading unmanned helicopter in the kth frame.

c) Initialize the location of the leading unmanned helicopter in the current frame as y_m. Calculate the distribution $\hat{p}_u(y_\mathrm{m})$ by (2).

d) Compute the new location y_1 of the leading unmanned helicopter by (9) and update the distribution $\hat{p}_u(y_1)$. If $d(y_1) < d(y_m)$, replace y_m with y_1.

e) If $\|y_1 - y_m\| < \varepsilon$ (ε is the threshold), replace the center of the leading unmanned helicopter $\hat{y}_k$ with the last y_1 and go to f). Otherwise, set $y_m = y_1$ and go to d).

f) Compute the log-polar transform of the leading unmanned helicopter in the kth frame using (30)–(33).

g) Compute the shifts $\Delta\xi^k,\ \Delta\psi^k$ between the log-polar transform of the leading unmanned helicopter in the first and current frames.

h) Compute S_k and r_k of the leading unmanned helicopter in the retinal plane by (34) and (35).

i) Update the tracking window of the leading unmanned helicopter with $\hat{y}_k$, S_k and r_k.

j) If the current frame is the last frame of the video, terminate the procedure. Otherwise, go to b).

6 Experimental results and discussion

To investigate the feasibility and efficiency of the proposed biologically MS-CPPBBO-SVR method, two sets of experiments were conducted. The competitive particle filter (PF) [27,28], MS, MS-SVR, MS with chaotic artificial bee algorithm [29] and SVR (MS-cABC-SVR), MS with chaotic particle swarm optimization (PSO) [30–33] and SVR (MS-cPSO-SVR), MS with BBO and SVR (MS-BBO-SVR) and MS-CPPBBO-SVR were used to track the leading unmanned helicopter in two video sequences to demonstrate the superiority of the proposed biologically MS-CPPBBO-SVR tracking method.

All of these tracking algorithms were encoded in Matlab 2010 and executed on a PC with 512 Mb RAM and running Windows XP. Based on tests and practical experience, the initial parameters of the different methods were set as follows. For CPPBBO and BBO, we set the population size $P = 20$, step size for numerical integration of the probabilities $dt = 1$, maximum migration rates $I = 1$, $E = 1$, and mutation probability $m = 0.08$. The number of elitisms was chosen as keep = 4. In addition, the adopted hunting rate was set to $\zeta = 0.03$ for the CPPBBO approach. Based on statistical data from tests for the convergence of each method using benchmark functions, the number of iterations of BBO was set to 30, and that of CPPBBO to 25 since the latter converges faster than basic BBO. The initial parameters of the cABC searching algorithm were set as: Ns = 60, Ne = 30, Nu = 30, and Limit = 5. The size of the population in the cPSO algorithm was 20, while the number of particles in the particle filter algorithm was set to 100. The Epanechnikov kernel function was used for the histogram computations. In addition, owing to the complexity of illuminating real-world scenes, the normalized RGB color space was taken as the feature space and quantized into $16 \times 16 \times 16$ bins.

The first video sequence consists of 150 frames, each with the size of 720×480. The leading unmanned helicopter was initialized with a green rectangular region of size 27×24 centered at $(349, 223)$ in the first frame. Some tracking results are shown in Figure 1.

Since the scale and orientation changes in the leading unmanned helicopter in this video sequence are very small at the beginning of tracking, the tracking results using MS-SVR are not very different from those of MS. When the leading unmanned helicopter speeds up suddenly, the performance of MS deteriorates in the latter few frames. Moreover, in the 115th and 129th frames, the tracking performance of MS-SVR is much worse than that of MS-cABC-SVR, MS-cPSO-SVR, MS-BBO-SVR, and MS-CPPBBO-SVR, but it is still better than the particle filter. The rectangles around the leading unmanned helicopter in the tracking results show that SVR allows the scale and orientation of the tracking windows to be self-adaptive.

To further prove the advantage of CPPBBO, the distance values of each method are presented in Figure 2. The distance value represents the difference between the target template and the target candidate. If the distance value of one frame is much greater than that of the first frame, the difference between the initial target template and the candidate of the current frame is greater. According to Figure 2, the distance value of MS increases as the number of frames increases up to 50, after which the value remains around 0.72, since it is caught in a local minimum; PF follows a similar pattern. The distance value of MS-CPPBBO-SVR in most cases is the smallest, which means that the proposed method is robust and adaptive.

To verify the robustness of our improved method, another video sequence with a more complex background and increased scale and orientation changes in the leading unmanned helicopter, was used in additional experiments. The second sequence has 300 frames with 320×160 pixels per frame. The leading unmanned helicopter was initialized with a rectangular region of size 24×21 centered at $(185, 105)$ in the first frame of the video sequence. Some tracking results are shown in Figure 3.

In tracking the leading unmanned helicopter in sequence 2, the environment for the flight is more complex than that in sequence 1 with trees and people included. These scenarios were set up to evaluate the performance of the tracking system under circumstance with interference. In this video sequence, when there are barriers or the leading unmanned helicopter speeds up, the tracking performance of MS-CPPBBO-SVR is the best owing to its adaptive tracking as well as the predator-prey mechanism that helps the primary algorithm escape from the local optima. MS and PF, on the other hand, fail to track the helicopter successfully. The scale and orientation of the tracking windows in methods using SVR are self-adaptive as shown in Figure 3.

Similar to the first video sequence, the distance values of different methods are given in Figure 4.

According to Figure 4, as the size and orientation of the movement of the leading unmanned helicopter change, the distance values vary from frame to frame; although, on the whole, they are increasing. The

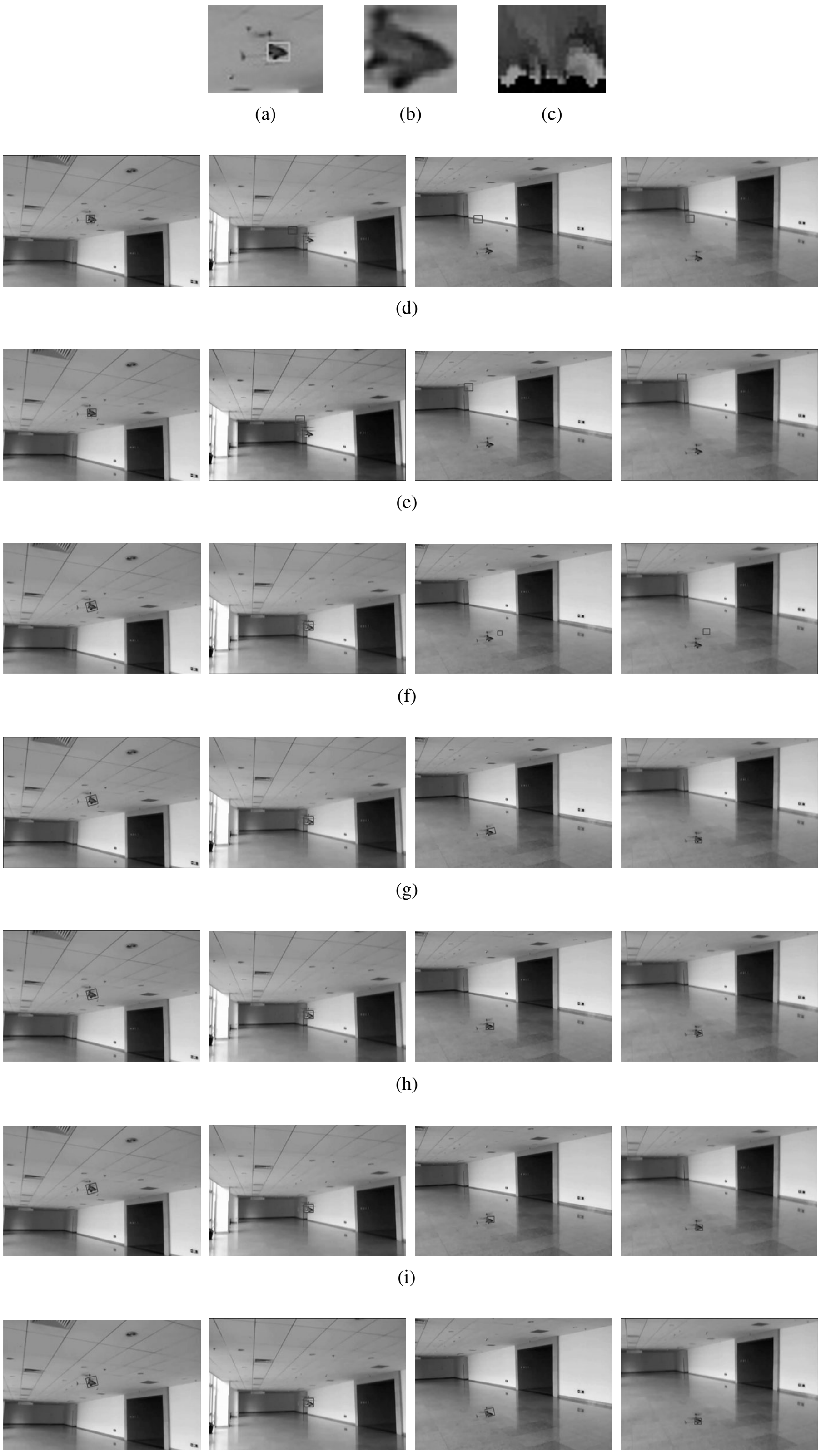

Figure 1 Tracking results of sequence 1: (a) target initialized in the first frame; (b) leading unmanned helicopter image; and (c) leading unmanned helicopter transformed to the cortical plane; Tracking results for the 20th, 60th, 115th, and 129th frames using (d) PF; (e) MS; (f) MS-SVR; (g) MS-cABC-SVR; (h) MS-cPSO-SVR; (i) MS-BBO-SVR; and (j) MS-CPPBBO-SVR.

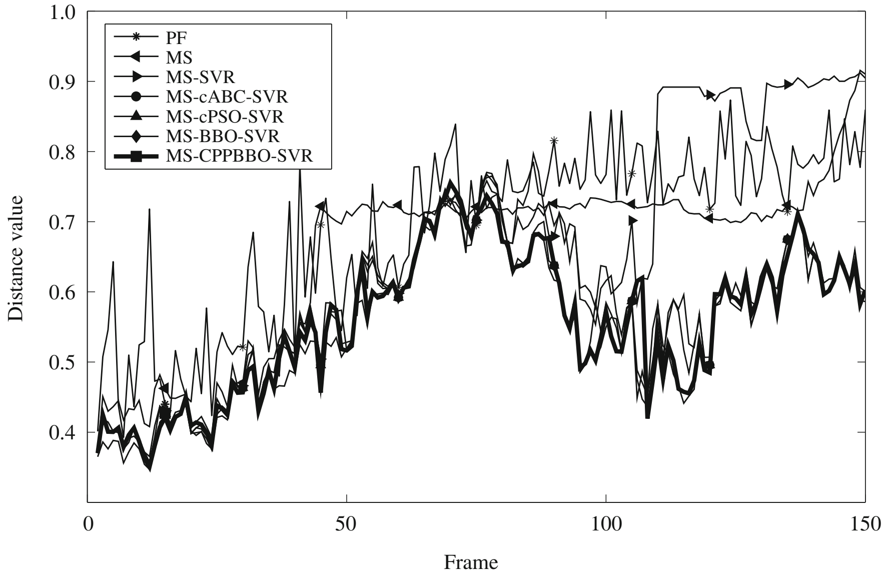

Figure 2 Distance values of the seven methods while tracking in sequence 1.

pulses of the curves are caused by size or orientation changes in the leading unmanned helicopter, an illumination change in the scene, or the leading unmanned helicopter being shadowed. In most frames, the distance value of the MS-CPPBBO-SVR algorithm is the smallest of all the curves, which means that the performance of MS-CPPBBO-SVR is the best in the tracking experiment. To highlight these results, the average distance values of the seven tracking methods are given in Table 1.

From Table 1, it is obvious that the average distance values of the MS-CPPBBO-SVR algorithm are the smallest of all the methods for both leading unmanned helicopter tracking experiments, which means that the performance of the proposed biologically MS-CPPBBO-SVR tracking method is the best. In sequence 1, the average distance value of the PF method is the largest, while in sequence 2, that of the MS method is the largest. Hence, the MS-CPPBBO-SVR algorithm is much more robust than the other methods. Considering that computation cost is very important for unmanned helicopter tracking and formation applications, we provide a table to compare the average time consumed for a single frame. Table 2 displays the comparative execution times of our proposed approach and the other six algorithms for twenty experiments in each case.

Table 2 shows that the execution timed of our proposed biologically MS-CPPBBO-SVR method are slightly longer than those of MS and MS-SVR, but shorter than those of the other four methods. More importantly, our method locates the leading unmanned helicopter more accurately than the two faster methods. It is very apparent when considering both the real-time criterion and the tracking results that our proposed biologically MS-CPPBBO-SVR is the most competitive method. In addition, SVR makes MS faster as it simplifies the tracking task as well as inhibits the impact of partial occlusions. The execution times of all the methods for sequence 2 are generally shorter than those for sequence 1owing to the actual quality of the videos.

7 Conclusion

In this paper we presented a novel biological approach, MS-CPPBBO-SVR, which can be used in UAV formation and conducted a series of experiments using video sequences with a leading unmanned helicopter. MS-CPPBBO-SVR enhances the performance of the classic MS tracking method as it combines basic MS with the CPPBBO algorithm and the SVR mechanism. In the MS-CPPBBO-SVR tracking method, the CPPBBO algorithm is used to search for a better target candidate for MS. The SVR mechanism is included to predict scale and rotation information of the target. Results of a series of comparative experi-

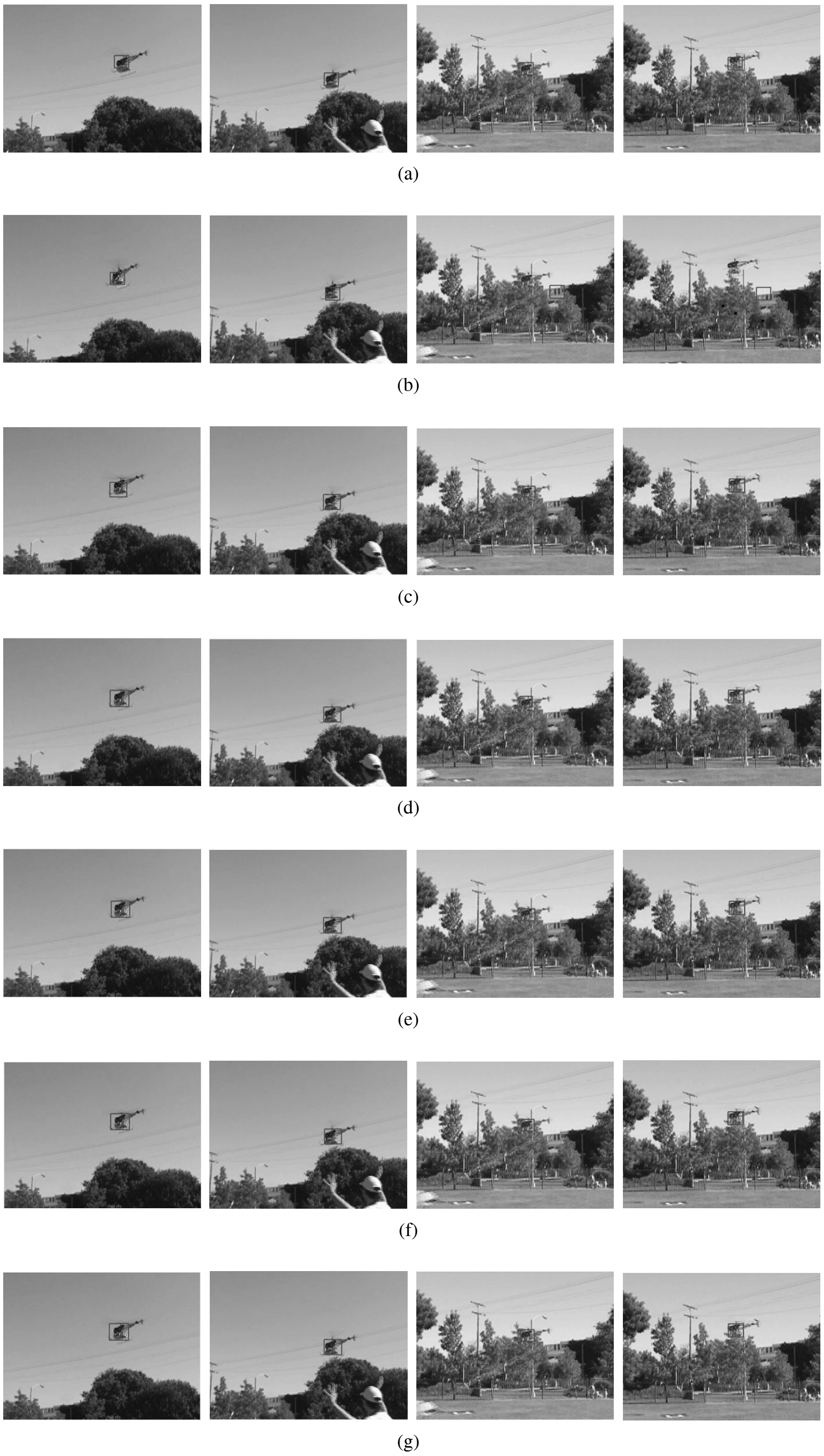

Figure 3 Tracking results for the 20th, 52th, 253th and 272th frames in sequence 2 using (a) PF; (b) MS; (c) MS-SVR; (d) MS-cABC-SVR; (e) MS-cPSO-SVR; (f) MS-BBO-SVR; and (g) MS-CPPBBO-SVR.

ments with other six other methods based on the leading unmanned helicopter were given to demonstrate the superiority of the proposed method.

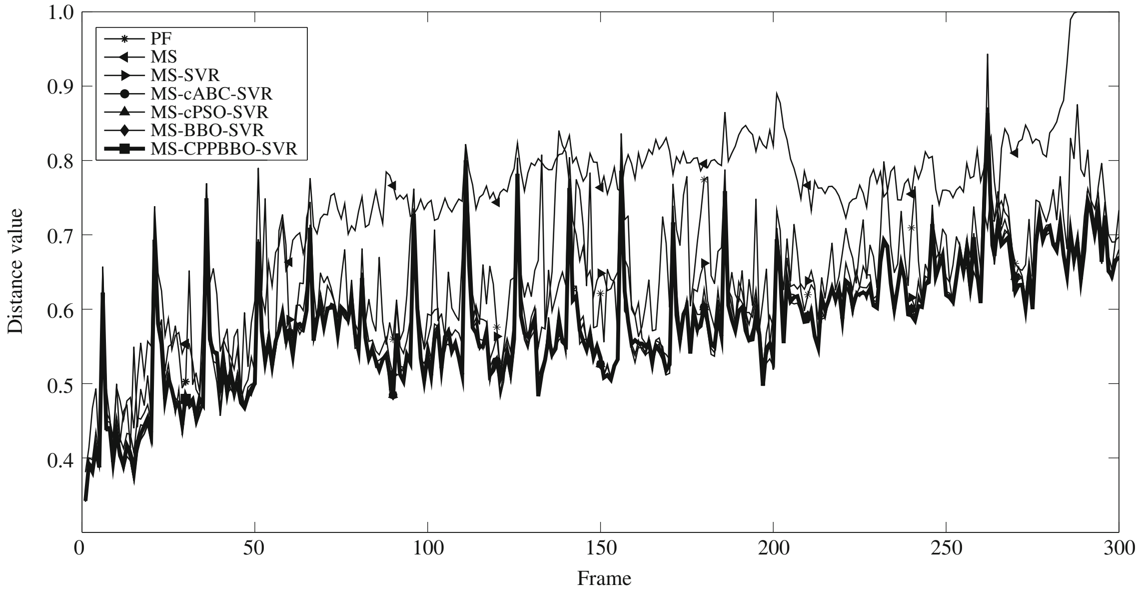

Figure 4 Distance values of the seven methods while tracking in sequence 2.

Table 1 Comparative results of average distance values

Algorithm	Sequence 1	Sequence 2
PF	0.6869	0.6436
MS	0.6541	0.7440
MS-SVR	0.6599	0.6032
MS-cABC-SVR	0.5658	0.5820
MS-cPSO-SVR	0.5588	0.5792
MS-BBO-SVR	0.5594	0.5818
MS-CPPBBO-SVR	0.5530	0.5704

Table 2 Comparative execution times for twenty experiments

Algorithm	Sequence 1 (s)	Sequence 2 (s)
PF	0.0902	0.0875
MS	0.0635	0.0360
MS-SVR	0.0424	0.0285
MS-cABC-SVR	0.0974	0.0847
MS-cPSO-SVR	0.1023	0.0881
MS-BBO-SVR	0.0792	0.0761
MS-CPPBBO-SVR	0.0773	0.0714

Acknowledgements

This work was partially supported by National Natural Science Foundation of China (Grant Nos. 61333004, 61273054, 61175109), Top-Notch Young Talents Program of China, and National Basic Research Program of China (973) (Grant No. 2014CB046401).

References

1 Lin F, Lum K Y, Chen B M, et al. Development of a vision-based ground target detection and tracking system for a small unmanned helicopter. Sci China Ser F-Inf Sci, 2009, 52: 2201–2215
2 Duan H B, Zhang Y P, Liu S Q. Multiple UAVs/UGVs heterogeneous coordinated technique based on Receding Horizon Control (RHC) and velocity vector control. Sci China Tech Sci, 2011, 54: 869–876
3 Duan H B, Luo Q N, Ma G J, et al. Hybrid particle swarm optimization and genetic algorithm for multi-UAV formation reconfiguration. IEEE Comput Intell Mag, 2013, 8: 16–27
4 Zhang X Y, Duan H B, Yu Y X. Receding horizon control for multi-UAVs close formation control based on differential evolution. Sci China Inf Sci, 2010, 53: 223–235
5 Duan H B, Liu S Q. Nonlinear dual-mode receding horizon control for multiple UAVs formation flight based on chaotic particle swarm optimization. IET Contr Theor Appl, 2010, 4: 2565–2578
6 Li J R, Li H Y, Tang G J. Optimal multi-objective trajectory design based on close-looped control for autonomous rendezvous. Sci China Tech Sci, 2011, 54: 3091–3097
7 Duan H B, Li P. Progress in control approaches for hypersonic vehicle. Sci China Tech Sci, 2012, 55: 2965–2970
8 Duan H B, Luo Q N, Yu Y X. Trophallaxis network control approach to formation flight of multiple unmanned aerial vehicles. Sci China Tech Sci, 2013, 56: 1066–1074

9 Cai G W, Chen B M, Peng K M, et al. Modeling and control of the yaw channel of a UAV helicopter. IEEE Trans Ind Electron, 2008, 55: 3426–3434
10 Peng K M, Dong M B, Chen B M. Design and implementation of a fully autonomous flight control system for a UAV helicopter. In: Proceedings of the 26th Chinese Control Conference, Zhangjiajie, 2007. 662–667
11 Wang R, Xia P Q. Control of dynamic stall of helicopter rotor blades. Sci China Tech Sci, 2013, 56: 171–180
12 Wang G L, Xia H, Yuan X M, et al. Modeling the yaw dynamics of an unmanned helicopter through modes partition method. Sci China Tech Sci, 2012, 55: 182–192
13 Fukanaga K, Hostetler L D. The estimation of the gradient of a density function, with applications in pattern recognition. IEEE Trans Inf Theory, 1975, 21: 32–40
14 Zhang C L, Jing Z L, Jin B, et al. A dual-kernel-based tracking approach for visual target. Sci China Inf Sci, 2012, 55: 566–576
15 Ning J, Zhang L, Zhang D, et al. Scale and orientation adaptive mean shift tracking. IET Comput Vis, 2012, 6: 52–61
16 Xiao G, Yun X, Wu J M. A multi-cue mean-shift target tracking approach based on fuzzified region dynamic mage fusion. Sci China Inf Sci, 2012, 55: 577–589
17 Wang C Y, Zhang H Q. An adaptive kernel bandwidth mean-shift target tracking algorithm. In: Proceedings of IEEE International Conference on Control Engineering and Communication Technology, Shenyang, 2012. 547–550
18 Li Y. Adaptive mean shift using hybrid particle swarm algorithm. J Huazhong Univ Sci Technol, 2010, 38: 47–49
19 Duan H B, Shao S, Su B W, et al. New development thoughts on the bio-inspired intelligence based control for unmanned combat aerial vehicle. Sci China Tech Sci, 2010, 53: 2025–2031
20 Costa e Silva M A, Coelho L D S, Lebensztajn L. Multiobjective biogeography-based optimization based on predator-prey approach. IEEE Trans Magn, 2012, 48: 951–954
21 Schwartz E L, Christman D R, Wolf A P. Human primary visual cortex topography imaged via positron tomography. Brain Res, 1984, 294: 225–230
22 Simon D. Biogeography-based optimization. IEEE Trans Evol Comput, 2008, 12: 702–713
23 Comaniciu D, Ramesh V, Meer P. Kernel-based object tracking. IEEE Trans Patt Anal Mach Intell, 2003, 25: 564–576
24 Simon D, Ergezer M, Du D W. Markov models for biogeography-based optimization and genetic algorithms with global uniform recombination. IEEE Trans Syst Man Cybern Part B-Cybern, 2011, 41: 299–306
25 Yan L, Jiang J P. Convergence and escape capacity research of evolution learning strategies. Acta Automat Sin, 2005, 31: 873–880
26 Lorenz E N. Deterministic nonperiodic flow. J Atmos Sci, 1963, 20: 130–141
27 Chang C, Ansari R. Kernel particle filter for visual tracking. IEEE Signal Process Lett, 2005, 12: 242–245
28 Lin L K, Xu H, Sheng W D, et al. Multi-target state-estimation technique for the particle probability hypothesis densty filter. Sci China Inf Sci, 2012, 55: 2318–2328
29 Xu C F, Duan H B, Liu F. Chaotic artificial bee colony approach to uninhabited combat air vehicle (UCAV) path planning. Aerosp Sci Technol, 2010, 14: 535–541
30 Liu F, Duan H B, Deng Y M. A chaotic quantum-behaved particle swarm optimization based on lateral inhibition for image matching. Optik, 2012, 123: 1955–1960
31 Duan H B, Sun C H. Pendulum-like oscillation controller design for micro aerial vehicle with ducted fan based on LQR and PSO. Sci China Tech Sci, 2013, 56: 423–429
32 Zhang S H, Ou J P. BP-PSO-based intelligent case retrieval method for high-rise structural form selection. Sci China Tech Sci, 2013, 56: 940–944
33 Duan H B, Yu Y X, Zhao Z Y. Parameters identification of UCAV flight control system based on predator-prey particle swarm optimization. Sci China Tech Sci, 2013, 56: 012202